Creation of a vortex in a Bose-Einstein condensate by superradiant scattering

M. E. Taşgın,[1] Ö. E. Müstecaplıoğlu,[2] and L. You[3]
[1]*College of Optical Sciences and Department of Physics, The University of Arizona, Tucson, Arizona 85721, USA*
[2]*Department of Physics, Koç University, Sariyer, Istanbul TR-34450, Turkey*
[3]*Department of Physics, Tsinghua University, Beijing 100084, People's Republic of China*
(Received 12 March 2011; revised manuscript received 5 October 2011; published 21 December 2011)

The creation of a topological vortex by a superradiant scattering of a Laguerre-Gaussian (LG) beam off an atomic Bose-Einstein condensate (BEC) is theoretically investigated. It is shown that scattered superradiant radiation can be either in a Gaussian mode without angular momentum or in a LG mode with angular momentum. The conditions leading to these two qualitatively distinct regimes of superradiance are determined in terms of the width for the pump laser and the condensate size for the limiting cases where the recoil energy is both much smaller and larger than the atomic interaction energy.

DOI: 10.1103/PhysRevA.84.063628 PACS number(s): 03.75.Lm, 42.50.Ct, 42.50.Nn, 05.30.Jp

I. INTRODUCTION

In addition to the spin angular momentum, associated with the polarization [1], electromagnetic radiation can also carry orbital angular momentum (OAM), associated with its spatial mode structure [2], as for example in Laguerre-Gaussian (LG) beams [3]. An electromagnetic field can exhibit quantum entanglement between OAM states [4]. It was proposed [5] and demonstrated [6] that superpositions of photonic OAM states can be utilized for higher-dimensional quantum communication and in dense data storage applications [7,8].

The success of applications of optical OAM would benefit from an efficient light-matter interface with fast mechanism for exchanging significant angular momentum between photons and atoms. For a superfluid state such as an atomic Bose-Einstein condensate (BEC), OAM states translate into topological excitations [9–12], for example, as vortices or circulating modes on a surface [13]. The transfer of angular momentum involving LG-beam-induced vortices in atomic condensates has been studied both experimentally [9–12] and theoretically [14–16].

An ensemble of atoms optically driven above a threshold intensity can emit radiation in the form of a superradiant (SR) pulse, which is a dynamical phenomenon [17,18]. In the case of equilibrium, Dicke SR is a first-order phase transition (PT) [19,20]. Early work on BEC SR [21–25] analyzed dynamical BEC SR in terms of matter-wave gratings in the translational [21–24,26,27] and in the polarization [25,28] degrees of freedom of the atoms. More recently, several authors discussed and demonstrated equilibrium Dicke SR and simultaneous structural PT from a homogenous to supersolid phase in a BEC trapped in an optical cavity [29,30], again restricted to translational degrees of freedom. The missing piece in the full puzzle of BEC SR and related studies is the rotational degrees of freedom. In this article we wish to consider a different type of SR beyond translational (linear momentum) and polarization (spin) degrees of freedom and discuss rotational degrees of freedom for both the optical and the matter fields. By considering superradiant scattering of an incident LG pump laser off the BEC, a sudden and complete transfer of OAM to the BEC brings it into a vortex state. Unlike the Raman coupled two-pulse pumping scheme of Refs. [10,11], this scheme yields a several orders of magnitude larger vortex/no-vortex recoil ratio (ratio of the occupation of the side mode with vortex to the occupation of the side mode without vortex). In addition to the rapid and efficient creation of vortexes, the recoiled atoms remain in the same internal state [11].

II. MODEL SYSTEM

We consider a cigar-shaped BEC in a nonrotating elongated trap, pumped by a far off-resonant intense laser field of momentum $\mathbf{k}_0$, collinear with the long condensate axis (z axis). For a Fresnel number close to unity the atoms collectively recoil into well-defined momentum states (side modes) [26], while the scattered light is predominantly along two end-fire modes propagating along $\pm z$, as depicted in Fig. 1.

After adiabatic elimination of the excited states, the effective Hamiltonian describing the interaction of the condensate atoms of transition frequency ω_a with an optical field of frequency ω_0 far detuned from the atomic transition by $\Delta = \omega_a - \omega_0$ is

$$\begin{aligned}\hat{\mathcal{H}} = &\int d^3\mathbf{r}\hat{\psi}^\dagger(\mathbf{r})\hat{H}_{\rm g}(\mathbf{r})\hat{\psi}(\mathbf{r}) + \sum_\ell \int d^3\mathbf{k}\hbar\omega_k \hat{a}^\dagger_{\mathbf{k},\ell}\hat{a}_{\mathbf{k},\ell} \\ &+ \sum_{\ell\ell'}\int d^3\mathbf{r}d^3\mathbf{k}d^3\mathbf{k}'\tilde{g}_{\ell\ell'}(\mathbf{k},\mathbf{k}';\mathbf{r})\hat{\psi}^\dagger(\mathbf{r})\hat{a}^\dagger_{\mathbf{k},\ell}\hat{a}_{\mathbf{k}',\ell'}\hat{\psi}(\mathbf{r}) \\ &+ \frac{g_s}{2}\int d^3\mathbf{r}\hat{\psi}^\dagger(\mathbf{r})\hat{\psi}^\dagger(\mathbf{r})\hat{\psi}(\mathbf{r})\hat{\psi}(\mathbf{r}), \end{aligned} \tag{1}$$

where $\hat{H}_{\rm g}(\mathbf{r})$ is the atomic Hamiltonian, $\hat{\psi}(\mathbf{r})$ is the annihilation operator for atoms in their electronic ground state, and $\hat{a}_{\mathbf{k},\ell}$ are optical field mode annihilation operators, the indices $\ell,\ell' = 0, \pm 1$ labeling the angular momentum of the optical modes [3]. The restrictive set of OAM is chosen in accordance with the angular momentum conservation and our choice of initial BEC and driving LG beam states.

The effective coupling coefficients

$$\tilde{g}_{\ell\ell'}(\mathbf{k},\mathbf{k}';\mathbf{r}) = -\frac{\hbar g^*(\mathbf{k})g(\mathbf{k}')}{\Delta}\Phi^*_{\mathbf{k},\ell}(\mathbf{r})\Phi_{\mathbf{k}',\ell'}(\mathbf{r}) \tag{2}$$

are determined by the single atom-photon dipole matrix element $g(\mathbf{k})$. Here $\Phi_{\mathbf{k},\ell}(\mathbf{r})$ are the mode functions of the light field with wave number $\mathbf{k}$ and angular momentum $\hbar\ell$.

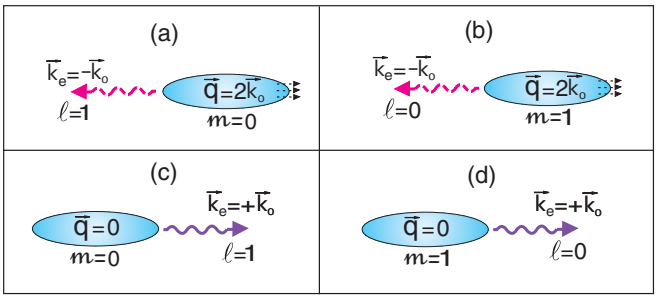

FIG. 1. (Color online) Cigar-shaped BEC initially in the state $m = 0, \mathbf{q} = 0$ and illuminated by a strong LG-mode laser of wave vector $\hbar\mathbf{k}_0$ and in the OAM mode $\ell = 1$. Superradiant scattering is predominantly along the end-fire modes with wave vector $\mathbf{k_e} = \pm\mathbf{k_0}$. Four possible end-fire modes and the corresponding matter-wave side modes are shown in (a)–(d).

Assuming the LG beam is well collimated over the long axis of the condensate and taking the radial mode number to be zero, LG modes are characterized only by their winding number l so that [15]

$$\Phi_{\mathbf{k},\ell}(\mathbf{r}) = \frac{1}{\sqrt{\pi l!}}\left(\frac{r}{w_L}\right)^{\ell} e^{-r^2/2w_L^2} e^{i\ell\phi} e^{ikz}, \tag{3}$$

of width w_L, which carries $\ell\hbar$ units of OAM along the z axis.

When driven by a Gaussian beam of wave vector $\mathbf{k}_0$, superradiant scattering occurs mainly in two counterpropagating end-fire modes of wave vectors $\mathbf{k} \simeq \pm\mathbf{k}_0$, where $\mathbf{k}_0$ is the wave vector of the pump photon. [22,23], with the initial condensate coupled to two dominant matter-wave side modes of momenta $\mathbf{q} = 0$ and $\mathbf{q} = 2\mathbf{k}_0$. With a LG driving field, in contrast, four end-fire optical modes are excited, with $\mathbf{k} \simeq \pm\mathbf{k}_0$ and $\ell = 0$ or 1, accompanied by four matter-wave side modes $\mathbf{k} \simeq \pm\mathbf{k}_0$ with $m = 1$ or 0, the optical end-fire modes with $\ell = 0$ being coupled to matter-wave modes with $m = 1$ due to conservation of angular momentum. It is the competition between these scattering channels that can result in the formation of a matter-wave vortex of "charge" $m = 1$ in the BEC (see Fig. 1).

III. TWO RECOIL REGIMES

The dynamics of scattering from a superfluid BEC fundamentally differs in two regimes determined by the relative strength of the recoil energy with respect to two-body interactions. If the recoil energy $[\hbar\omega_R(q) = \hbar^2q^2/2M]$ is much smaller than the interparticle interaction energy (per atom), $\hbar\omega_R \ll U_{\rm int}$, excitations are highly suppressed [11,31,32]. The interparticle interaction leads to a collective response to the rotational effect by the incident LG beam. In this regime, the condensate can be described with a single wave function (order parameter) within the mean-field theory.

For relatively large recoil energy $\hbar\omega_R \gg U_{\rm int}$ atoms can scatter and group into independent recoil modes (side modes) [10,11,21–23]. In this regime BEC can be described in terms of a collection of relevant side-modes as illustrated in Fig. 1. There are typical experiments [10] in this regime where partial recoil of the condensate into a vortex mode cannot be described by a single wave function, with vortex core on the axis [13], but rather resembles a two-component BEC. Each of the components can have different wave functions (mode profiles) [33]. In our treatment of the large recoil regime, we follow a similar approach but for three-component condensate. We use approximate frozen profiles of the condensate modes to make analytical calculations of quantum dynamics, by ignoring atom-atom collisions in this regime. In our treatment of the small recoil regime, we solve classical mean-field dynamics of condensates coupled to end-fire modes.

1. Large recoil-energy regime

Since the large recoil-energy regime corresponds to a series of well-known experiments [21–23], we investigate it first. It is known that superradiance in an atomic BEC can be modeled by an effective Hamiltonian that only includes the dominant end-fire modes of the light field and the associated matter-wave side modes [15,26,34]. We can then proceed by expanding the condensate field operator in terms of side modes [26] as

$$\hat{\psi}_{\rm g}(\mathbf{r}) = \sum_{m,q_z} \varphi_{m,q_z}(\mathbf{r})\hat{c}_{q_z,m}, \tag{4}$$

where $\varphi_{m,q_z}(\mathbf{r}) = \varphi_m(r)e^{im\phi}e^{iq_zz}$ is the eigenfunction of an atom with recoil momentum q_z in the z direction and vortex charge m. It is given by the solution of the single-particle equation $\hat{H}_m(r)\varphi_m(r) = \Omega_m\varphi_m(r)$, where

$$\hat{H}_m(\mathbf{r}) = \frac{-\hbar^2}{2M}\left(\frac{d^2}{dr^2} + \frac{1}{r}\frac{d}{dr}\right) + \frac{m^2\hbar^2}{2Mr^2} + V_t(\mathbf{r}), \tag{5}$$

and V_t is the trap potential. Two-body interactions are negligible in the large recoil regime [15]. For a harmonic trap, these states are similar to the LG modes [15]

$$\varphi_m(r) = \frac{1}{\sqrt{m!\pi w^2}}\left(\frac{r}{w}\right)^m e^{-r^2/2w^2}, \tag{6}$$

where w is the radial width of the condensate.

Focusing on first-order scattering processes reduces the Hamiltonian of the system to the simplified form

$$\hat{\mathcal{H}} = \sum_{m,q_z}\epsilon_m(q_z)\hat{c}^\dagger_{q_z,m}\hat{c}_{q_z,m} + \sum_{\ell}\int d^3\mathbf{k}\hbar\omega_k\hat{a}^\dagger_{\mathbf{k},\ell}\hat{a}_{\mathbf{k},\ell} + \sum_{\ell,m,q_z}\int dk_z g_{\ell m}(k_z,q_z)\hat{c}^\dagger_{q_z,m}\hat{a}^\dagger_{k_z,l}\hat{a}^{(L)}_{k_0,1}\hat{c}_{0,0} + \text{H.c.}, \tag{7}$$

where $\epsilon_m(q_z) = \hbar[\Omega_m + \omega_R(q_z)]$, $\hat{a}^{(L)}_{k_0,1}$ is the LG pump laser mode, $\hat{c}_{0,0}$ describes the initial condensate, and

$$g_{\ell m}(k_z,q_z) = -\hbar\frac{g^*(k_z)g(k_0)}{\Delta}\delta_{\ell+m,1} \times \int d^3\mathbf{r}\varphi^*_{q_z,m}(\mathbf{r})\Phi^*_{k_z,\ell}(\mathbf{r})\Phi_{k_0,1}(\mathbf{r})\varphi_{0,0}(\mathbf{r}). \tag{8}$$

When driven by a Gaussian beam of wave vector $\mathbf{k}_0$, superradiant scattering occurs mainly in two counterpropagating end-fire modes of wave vectors $\mathbf{k} \simeq \pm\mathbf{k}_0$, where $\mathbf{k}_0$ is the wave vector of the pump photon [22,23], with the initial condensate coupled to two dominant matter-wave side modes of momenta $\mathbf{q} = 0$ and $\mathbf{q} = 2\mathbf{k}_0$. With a LG driving field four end-fire optical modes are excited, with $\mathbf{k} \simeq \pm\mathbf{k}_0$ and $\ell = 0$ or 1, accompanied by four matter-wave side modes $\mathbf{k} \simeq \pm\mathbf{k}_0$ with $m = 1$ or 0, the optical end-fire modes with $\ell = 0$ being

coupled to matter-wave modes with $m = 1$ due to conservation of angular momentum (see Fig. 1).

In the large recoil-energy regime, rotatory forward scattering [Fig. 1(d)] of LG laser is neglected on the basis that (i) it cannot transfer sufficient linear momentum and excitation energy [31,32] and (ii) such low-energy scattering is suppressed by the structure factor of the BEC [31,35]. The process described in Fig. 1(c) is neglected as it is not a superradiant process, but just the forward scattering into the pump mode that leads to a phase shift. Keeping only relevant modes results in the effective Hamiltonian ($\hbar = 1$)

$$\begin{aligned}\hat{\mathcal{H}}_{\rm int} = &-\left(g_1\hat{c}^\dagger_{2k_0,0}\hat{a}^\dagger_{-k_0,1}\hat{a}^{(L)}_{k_0,1}\hat{c}_{0,0} + \text{H.c.}\right)\\ &-\left(g_2\hat{c}^\dagger_{2k_0,1}\hat{a}^\dagger_{-k_0,0}\hat{a}^{(L)}_{k_0,1}\hat{c}_{0,0} + \text{H.c.}\right),\end{aligned} \tag{9}$$

where $\hat{c}_{2k_0,0}$, $\hat{c}_{2k_0,1}$, $\hat{a}_{-k_0,1}$, and $\hat{a}_{-k_0,0}$ are the matter-wave side modes and optical end-fire modes illustrated in Figs. 1(a) and 1(b). Here $g_1 \equiv g_{10}$ and $g_2 \equiv g_{01} = (w_L/w)g_1$ can be calculated from Eq. (8), consistently with Ref. [15]. The free-field terms have been eliminated through a second rotating frame transformation after moving to a corotating frame at the laser frequency [34]. The first term in Eq. (9) yields normal (nonrotatory) SR, while the second term induces vortex excitations in the BEC and results in rotatory SR.

For times short enough that the depletion of the initial condensate can be ignored, we can make the substitution $\hat{c}_{0,0} \to \sqrt{N}$, where N is the number of condensed atoms. In that limit the side-mode population dynamics can be treated analytically [26], giving $d\hat{c}_{2k_0,m}/dt \simeq G_m N \hat{c}_{2k_0,m}/2$, with $G_m \propto g^2_{m+1}$. For $g_2/g_1 = w_L/w \gtrsim 1$, the initial exponential growth of vortex side-mode occupation from initial fluctuations is faster than that of the nonvortex side mode. This suppresses normal SR relative to rotatory SR and leads to a topological vortex regarding the occupation dynamics [34]. For example, a typical ratio $g_2/g_1 = 2$ [10] would result in vortex/no-vortex side mode population ratio of 3×10^4 for $N = 10^6$. We note that the condition $w_L \gtrsim w$ is consistent with OAM transfer into classical objects [36] and with the two-pump Raman vortex excitation protocol in BEC [10]. In these cases, however, the resulting vortex/no-vortex population ratio increases linearly with $(w_L/w)^2$, in contrast to the exponential growth characteristic of the present situation.

2. *Small recoil-energy regime*

To investigate the small recoil-energy regime, we include the effects of two-body collisions and we invoke the mean-field approximation whereby the field operators are replaced by c numbers, $\hat{\psi} \to \psi$, $\hat{a}_{-k_0,1} \to \alpha_1$, $\hat{a}_{-k_0,0} \to \alpha_2$, $\hat{a}_{k_0,0} \to \alpha_3$, and $\hat{a}^{(L)}_{k_0,1} \to \alpha_L$, without side-mode expansion (4). In the small recoil regime, where single-atom scattering is already forbidden [11,31,35], all processes [Figs. 1(a)–1(d)] contribute. The Heisenberg equations of motion reduce to a Gross-Pitaevskii equation for the condensate wave function coupled to three optical fields so that

$$\begin{aligned}i\dot{\psi} = &\hat{H}_g\psi - 2U_0[|\alpha_L|^2\left|\Phi_{k_0,1}\right|^2 + |\alpha_1|^2\left|\Phi_{-k_0,1}\right|^2\\ &+|\alpha_2|^2|\Phi_{-k_0,0}|^2 + |\alpha_3|^2|\Phi_{k_0,0}|^2]\psi\\ &-U_0\alpha_L[\alpha_1^*\Phi^*_{-k_0,1}\Phi_{k_0,1} + \alpha_2^*\Phi^*_{-k_0,0}\Phi_{k_0,1}\\ &+\alpha_3^*\Phi^*_{k_0,0}\Phi_{k_0,1} + \text{c.c.}]\psi + g_S|\psi|^2\psi,\end{aligned} \tag{10}$$

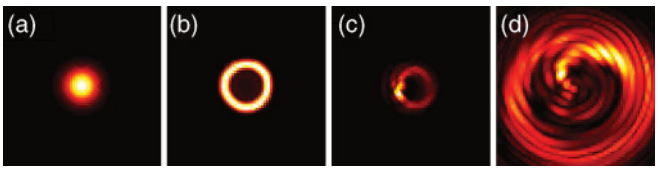

FIG. 2. (Color online) Snapshots of radial density profile of BEC at different times during the interaction by a LG laser beam. (A) The BEC starts in a Gaussian state ($\omega_R t = 0$). (B) Onset of normal SR, with the condensate density mapping the LG intensity profile, but with zero average OAM ($\omega_R t = 8$). (C) Just before the onset of rotatory SR the axial ϕ symmetry of the condensate is broken, with a higher density near the $\phi \simeq \pi$ angle ($\omega_R t = 33$). (D) Rotatory SR induces a vortex in the BEC, when $\langle L_z\rangle$ jumps from 0 to $N\hbar$. As time progress, the circulation broadens into a swirling pattern ($\omega_R t = 45$).

$$i\dot{\alpha}_1 = -\Delta_1\alpha_1 - 2U_0 I^{1,1}_{-,-}\alpha_1 - U_0\alpha_L I^{1,1}_{-,+}, \tag{11}$$

$$i\dot{\alpha}_2 = -\Delta_2\alpha_2 - 2U_0 I^{0,0}_{-,-}\alpha_2 - U_0\alpha_L I^{0,1}_{-,+}, \tag{12}$$

$$i\dot{\alpha}_3 = -\Delta_3\alpha_3 - 2U_0 I^{0,0}_{+,+}\alpha_3 - U_0\alpha_L I^{0,1}_{+,+}. \tag{13}$$

Here $U_0 = g^2/\Delta$, $g_S = 4\pi\hbar a_s/m$, a_s being the s-wave scattering length, $-\Delta_{1,2,3}$ are the end-fire mode frequencies in the rotating frame at frequency ω_0, and

$$I^{m,m'}_{\alpha,\beta} = \int d^3\mathbf{r}\Phi^*_{\alpha k_0,m}(\mathbf{r})\Phi_{\beta k_0,m'}(\mathbf{r})\,|\psi(\mathbf{r},t)|^2\,, \tag{14}$$

where α and $\beta = \pm 1$ label the sign of the wave vectors of amplitude k_0. We assume no particular loss mechanism is in effect.

Figures 2 and 3 summarize the results of a typical numerical solution of these equations. In this example $w_L = 1.2w$, $NU_0 = 10$, $\eta = \alpha_L\sqrt{N}U_0 = 15$, $\Delta_1 = 1$, $\Delta_2 = 1.001$, and $\Delta_3 = 10^{-3}$ in units of the recoil frequency ω_R. These values are comparable to those of Refs. [21,30].

The results of our simulation illustrated in Fig. 2 show four snapshots of the transition from a stationary Gaussian BEC to a rotating vortex BEC. Figure 2(A) shows the initial condensate in the ground state of the harmonic trap. At the onset of normal SR, as shown in Fig. 2(B), condensate density profile maps the intensity profile of the driving LG beam, but still with zero average angular momentum. The effect of α_1 on the BEC profile can be interpreted by an effective potential,

$$V_1 = -U_0\left[2\left|\Phi_{-k_0,1}\right|^2 + \left(\alpha_L\alpha_1\phi^*_{-k_0,1}\phi_{k_0,1} + \text{c.c.}\right)\right]. \tag{15}$$

This forces BEC into the ring profile in Fig. 2(B). Through the overlap integrals, that particular profile further enhances α_1. As such, the effective potential becomes deeper and deeper while the ring gets denser and thinner. The ring profile becomes more susceptible to fluctuations so that at a certain point it loses its azimuthal uniformity. Fluctuations exist in numerical simulations as well as in initial seeding of the optical modes. The axial symmetry is broken in Fig. 2(C), where accumulation of density peak near $\phi \sim \pi$ can be seen. Following the rotational symmetry breaking, a rotatory condensate is formed, carrying one quantum of angular momentum per atom; that is, a condensate in a vortex state appears as in Fig. 2(D). The swirling vortex profile now favors the α_3 mode, which is simultaneously scattered off the

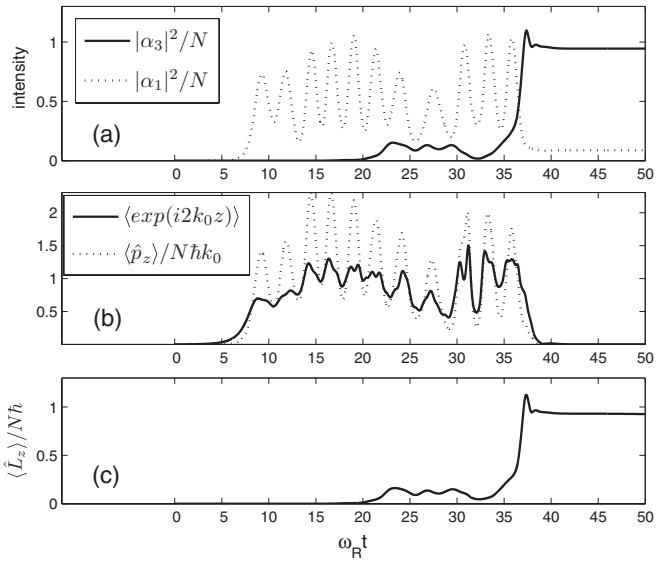

FIG. 3. Time evolution of the condensate for the parameters of Fig. 2. All the quantities plotted are dimensionless. (a) Mean photon number in the Gaussian end-fire mode $|\alpha_3|^2$ and in the LG end-fire mode. (b) Linear momentum transfer ($\langle p_z\rangle \propto |\alpha_1|^2$) and expectation value of the two-photon momentum recoil operator $\langle e^{2ik_0z}\rangle$. (c) Expectation value of the normalized angular momentum $\langle\hat{L}_z\rangle/N\hbar$.

vortex as rotatory SR. Similarly, rotation experiments using classical objects reveal [36] that higher OAM is transferred to materials with higher ϕ-anisotropic density. A related situation occurs in the self-organization into even-odd lattice sites by translational symmetry breaking in the Dicke superradiance of a BEC in a cavity QED setting [29].

The dynamics of the transition are shown in more detail in Fig. 3, which plots the evolution of key observables during the SR transition to the vortex state: For the parameters of these simulations the normal SR happens at $t \simeq 8/\omega_R$ [Fig. 2(b)]. It coincides with the peak of $|\alpha_1|^2$ in Fig. 3(a). Spatial order sets in along the z direction, as can be seen in Fig. 3(b), as evidenced by the nonzero value of $\langle e^{2ik_0z}\rangle$. The condensate acquires linear momentum $\langle\hat{p}_z\rangle/\hbar k_0 = 2|\alpha_1|^2$ as a result of momentum conservation (note that $\alpha_2 = 0$). In this early stage, there is no OAM transfer to the condensate. Both the laser and the end-fire modes have equal winding number $\ell = 1$.

This early dynamics is followed by the onset of rotatory SR. As a precursor to that transition the condensate first exhibits an axial symmetry breaking, as in Fig. 2(C). This is the indication of OAM transfer from the optical field to the atoms. Rotatory SR reveals itself with a sudden increase in the intensity $|\alpha_3|^2$, shown in Fig. 3(a), and a decrease in the LG mode $|\alpha_1|^2$. At this point the angular momentum is transferred fully from the optical field to the matter wave, establishing a vortex in the BEC [Fig. 2(d)], the BEC gaining $\langle\hat{L}_z\rangle = N\hbar$ [Fig. 3(c)] of OAM. A comparison of Figs. 3(a) and 3(c) indicates that the total OAM of the system is conserved in this transition, during which the process the linear momentum along z is transferred back to the optical field, as can be seen from Figs. 3(a) and 3(b).

We finally remark that we found, by numerical analysis, that the critical pump rates (η) are different for the onset of nonrotatory ($\eta_1 = 9.5$) [20,29,30] and rotatory SR ($\eta_2 = 12.4$): Below η_1 no SR scattering occurs. Between the two values ($\eta_1 < \eta < \eta_2$) only normal SR takes place, and rotatory SR occurs for above η_2.

IV. CONCLUSIONS

Summarizing, we have examined theoretically the mutual induction of a topological vortex in a BEC and a rotatory SR. The cooperative nature of SR from an incident LG laser beam allows for a sudden transfer of a large amount of OAM into a condensate, bringing it into a vortex state. For most current condensate SR experiments, nonrotatory SR can be exponentially suppressed by rotatory SR if the transverse width of the LG pump laser is larger than the condensate transverse width.

ACKNOWLEDGMENTS

The question of the influence of a LG pump on BEC SR was raised by L. Deng. We are grateful to him for his insight and for bringing this question to our attention. We thank P. Meystre for illuminating discussions. Ö.E.M. and M.E.T. acknowledge D.P.T. (T.R. Prime Ministry State Planning Organization) National Quantum Cryptology Center, TUBITAK 2219 program, and TUBITAK Project No. 109T267 for support.

[1] R. A. Beth, Phys. Rev. **48**, 471 (1935); **50**, 115 (1936).
[2] C. Cohen-Tannoudji, J. Dupont-Roc, and G. Grynberg, *Photons and Atoms* (Wiley, New York, 1989).
[3] L. Allen, M. W. Beijersbergen, R. J. C. Spreeuw, and J. P. Woerdman, Phys. Rev. A **45**, 8185 (1992).
[4] A. Mair, A. Vaziri, G. Weihs, and A. Zeilinger, Nature (London) **412**, 313 (2001).
[5] G. Molina-Terriza, J. P. Torres, and L. Torner, Phys. Rev. Lett. **88**, 013601 (2001).
[6] G. Molina-Terriza, A. Vaziri, J. Rehacek, Z. Hradil, and A. Zeilinger, Phys. Rev. Lett. **92**, 167903 (2004); G. Molina-Terriza, J. P. Torres, and L. Torner, Nat. Phys. **3**, 305 (2007).
[7] D. Kaszlikowski, P. Gnacinski, M. Zukowski, W. Miklaszewski, and A. Zeilinger, Phys. Rev. Lett. **85**, 4418 (2000).
[8] D. Collins, N. Gisin, N. Linden, S. Massar, and S. Popescu, Phys. Rev. Lett. **88**, 040404 (2002).
[9] J. W. R. Tabosa and D. V. Petrov, Phys. Rev. Lett. **83**, 4967 (1999).
[10] M. F. Andersen, C. Ryu, P. Clade, V. Natarajan, A. Vaziri, K. Helmerson, and W. D. Phillips, Phys. Rev. Lett. **97**, 170406 (2006).
[11] K. C. Wright, L. S. Leslie, and N. P. Bigelow, Phys. Rev. A **77**, 041601(R) (2008).
[12] D. Moretti, D. Felinto, and J. W. R. Tabosa, Phys. Rev. A **79**, 023825 (2009).

[13] C. J. Pethick and H. Smith, *Bose-Einstein Condensation in Dilute Gases* (Cambrige University Press, Cambridge, 2002), p. 250.
[14] K.-P. Marzlin, W. Zhang, and E. M. Wright, Phys. Rev. Lett. **79**, 4728 (1997).
[15] R. Kanamoto, E. M. Wright, and P. Meystre, Phys. Rev. A **75**, 063623 (2007).
[16] Z. Dutton and J. Ruostekoski, Phys. Rev. Lett. **93**, 193602 (2004); S. Thanvanthri, K. T. Kapale, and J. P. Dowling, Phys. Rev. A **77**, 053825 (2008).
[17] R. H. Dicke, Phys. Rev. **93**, 99 (1954).
[18] N. Skribanowitz *et al.*, Phys. Rev. Lett. **30**, 309 (1973).
[19] Y. K. Wang and F. T. Hioe, Phys. Rev. A **7**, 831 (1973); K. Hepp and E. H. Lieb, Ann. Phys. **76**, 360 (1973).
[20] C. Emary and T. Brandes, Phys. Rev. E **67**, 066203 (2003).
[21] S. Inouye *et al.*, Science **285**, 571 (1999).
[22] J. Li *et al.*, Phys. Lett. A **372**, 4750 (2008).
[23] L. Deng, M. G. Payne, and E. W. Hagley, Phys. Rev. Lett. **104**, 050402 (2010).
[24] L. Fallani, C. Fort, N. Piovella, M. Cola, F. S. Cataliotti, M. Inguscio, and R. Bonifacio, Phys. Rev. A **71**, 033612 (2005).
[25] D. Schneble, G. K. Campbell, E. W. Streed, M. Boyd, D. E. Pritchard, and W. Ketterle, Phys. Rev. A **69**, 041601(R) (2004).
[26] M. G. Moore and P. Meystre, Phys. Rev. Lett. **83**, 5202 (1999); O. E. Mustecaplioglu and L. You, Phys. Rev. A **62**, 063615 (2000).
[27] O. Zobay and G. M. Nikolopoulos, Phys. Rev. A **73**, 013620 (2006).
[28] H. Uys and P. Meystre, Phys. Rev. A **75**, 033805 (2007).
[29] K. Baumann, C. Guerlin, F. Brennecke, and T. Esslinger, Nature (London) **464**, 1301 (2010).
[30] D. Nagy, G. Szirmaia, and P. Domokos, Eur. Phys. J. D **48**, 127 (2008); P. Domokos and H. Ritsch, Phys. Rev. Lett. **89**, 253003 (2002).
[31] D. M. Stamper-Kurn, A. P. Chikkatur, A. Gorlitz, S. Inouye, S. Gupta, D. E. Pritchard, and W. Ketterle, Phys. Rev. Lett. **83**, 2876 (1999).
[32] R. Graham and D. Walls, Phys. Rev. Lett. **76**, 1774 (1996).
[33] Tin-Lun Ho, Phys. Rev. Lett. **81**, 742 (1998).
[34] M. E. Taşgin, M. O. Oktel, L. You, and O. E. Mustecaplioglu, Phys. Rev. A **79**, 053603 (2009).
[35] L. Deng and E. W. Hagley, Phys. Rev. A **82**, 053613 (2010).
[36] A. T. O'Neil, I. MacVicar, L. Allen, and M. J. Padgett, Phys. Rev. Lett. **88**, 053601 (2002).